

## Low-field magnetization of radio-frequency-sputtered $\text{Fe}_x\text{Zr}_{100-x}$ amorphous alloys: the magnetic phase diagram

This article has been downloaded from IOPscience. Please scroll down to see the full text article.

1997 J. Phys.: Condens. Matter 9 1609

(<http://iopscience.iop.org/0953-8984/9/7/022>)

View [the table of contents for this issue](#), or go to the [journal homepage](#) for more

Download details:

IP Address: 171.66.16.207

The article was downloaded on 14/05/2010 at 08:08

Please note that [terms and conditions apply](#).

# Low-field magnetization of radio-frequency-sputtered $\text{Fe}_x\text{Zr}_{100-x}$ amorphous alloys: the magnetic phase diagram

F J Castaño†, T Stobiecki‡, M R J Gibbs† and H J Blythe†

† Department of Physics, University of Sheffield, Sheffield S3 7RH, UK

‡ Department of Electronics, Academy of Mining and Metallurgy, Mickiewicza 30, 30-059 Cracow, Poland

Received 3 October 1996

**Abstract.** Magnetization measurements have been performed in the temperature range 5–300 K on amorphous  $\text{Fe}_x\text{Zr}_{100-x}$  ( $40 \leq x \leq 64$ ) samples prepared by rf sputtering. The decrease of the magnetization at low temperature and low applied field ( $\mu_0 H < 5$  mT) is interpreted as being evidence for the existence of a low-temperature, complex magnetic state in this composition range; a magnetic phase diagram is proposed.

## 1. Introduction

The magnetic properties of amorphous  $\text{Fe}_x\text{Zr}_{100-x}$  alloys have now constituted a major part of the research activity in the field of amorphous magnetism for more than a decade [1]. The liquid-quench and vapour-deposition techniques are most generally used to produce Fe–Zr amorphous alloys. A stable amorphous state exists for liquid-quench amorphous  $\text{Fe}_x\text{Zr}_{100-x}$  alloys only in two limited compositional ranges near the eutectic compositions  $85 \leq x \leq 93$  and  $20 \leq x \leq 50$  [2]. However, the rf [3] and DC [4, 5] sputtering techniques, due to much higher quenching rates, are able to produce amorphous  $\text{Fe}_x\text{Zr}_{100-x}$  alloys over a wider range of composition ( $20 \leq x \leq 93$ ).

These alloys exhibit drastically differing properties depending on their composition; this ranges from superconducting behaviour [2] for Fe-dilute alloys ( $x \leq 35$ ) to Invar and spin-glass characteristics [6–8] for Fe-rich samples ( $x \leq 88$ ). The magnetic moment per Fe atom ( $\mu$ ) as well as the Curie temperature ( $T_C$ ) seem each to have a maximum for an alloy with  $x = 80$  [9], although other workers [3] suggest that this maximum may lie nearer to  $x = 85$ . On increasing the Fe content above this concentration,  $\mu$  and  $T_C$  decrease up to  $x = 94.5$  [10]. Above this Fe concentration, a uniformly amorphous state has not been obtained; it is thought that alloys in this region behave as an array of non-interacting Fe clusters and hence no long-range magnetic order is established.

For Fe concentrations below  $x = 80$ ,  $T_C$  and  $\mu$  decrease, becoming equal to zero for an alloy with a value of  $x$  around  $x = 35$  [3]. The magnetization at  $T = 0$  K has been studied numerically using itinerant magnetism theory [11] and the rigid-band model [12, 13]. In the magnetic region,  $35 \leq x \leq 94.5$ , there is still some controversy as to the description of the ferromagnetic state to which the transition at  $T_C$  leads [14]. In addition to the transition at  $T_C$ , the magnetic properties of these amorphous alloys within the Fe-rich and the intermediate-concentration ( $35 \leq x \leq 45$ ) ranges appear to be further complicated by the possibility of a second, transverse spin-freezing transition at the temperature  $T_{xy}$ , below  $T_C$ .

Evidence of this second magnetic transition can be found in Mössbauer data [9] as well as thermo-magnetization measurements [5, 15], although these latter data do not indicate that the transition is spontaneous in the sense associated with a genuine thermodynamic phase transition, as the vector model predicts [16]. The exact determination of the temperature of this second transition and its interpretation are still unclear.

Magnetization measurements have been reported on rf-sputtered  $\text{Fe}_x\text{Zr}_{100-x}$  amorphous samples [3, 17] within the intermediate-concentration range ( $35 \leq x \leq 85$ ). These results show a very large high-field susceptibility for all samples, and that the contributions to the thermal demagnetization are determined only by spin-wave excitations and not by fluctuation of the exchange integral, as in the Fe-rich region. Further work, in terms of the magnetic state in this intermediate region, is still needed in order to provide a better understanding of the magnetic behaviour of these amorphous alloys. Up to the present time, systematic thermo-magnetization measurements, using a single production route, to establish the magnetic phase diagram have not been undertaken. Such measurements form part of this study.

Up to the present time, there have been various attempts to describe the low-temperature magnetic structures that are able to account for the properties of melt-spun amorphous alloys within the Fe-rich region [15]. Recent theoretical and experimental papers [18, 19] on  $\text{Fe}_x\text{Zr}_{100-x}$  amorphous alloys in the Fe-rich region suggest that only two models are still to be considered. The basic physical idea underlining both models is that, due to the fluctuation of the interatomic distance inherent in the amorphous structure, fluctuating positive and negative exchange interactions occur between neighbouring Fe atoms. This leads to a complex long-range-ordered magnetic state at low temperatures.

(a) The first model [15] describes the magnetic microstructure of melt-spun  $\text{Fe}_x\text{Zr}_{100-x}$  amorphous ribbons within the Fe-rich region as an array of small, single-domain, Fe-rich clusters (treated as an assembly of Néel interacting fine particles) that form a granular magnetic structure, which is not yet understood. This magnetic microstructure appears to be unique to  $\text{Fe}_x\text{Zr}_{100-x}$  amorphous alloys, and this cluster model has been supported by interpretation of Mössbauer measurements [20], which show an increase of the linewidth of the Mössbauer spectrum at around the temperature of the second transition,  $T_{xy}$ . This broadening is interpreted as evidence of cluster relaxation phenomena. This implies in turn that the temperature  $T_{xy}$  can be regarded as a cluster blocking temperature, although this type of granular magnetic structure cannot be described as a superparamagnet and so cannot be explained by currently accepted theories. A superparamagnetic (Langevin behaviour of the magnetization curves and coercivity disappearing above the blocking temperature) or cluster behaviour with a real phase separation between clusters would [21] predict discontinuities in the high-field susceptibility versus temperature plots in the vicinity of the blocking temperature. In the experimental high-field susceptibility data reported in the literature for these amorphous alloys, these discontinuities were not observed [15, 22, 23].

(b) In the second model [24], the increase of the linewidth in the Mössbauer spectrum at around  $T_{xy}$  is interpreted as an indication that this temperature can be considered as a transverse spin-freezing temperature. This is proposed as the Mössbauer spectrum can also be interpreted as indicating a non-collinear spin structure, consistent with the high-field susceptibility of these amorphous alloys, which fail to saturate even in fields up to 20 T. This model suggests that the magnetic structure of melt-spun samples in the Fe-rich region consists of a ferromagnetic structure in the temperature range  $T_{xy} < T < T_C$ , with evidence of transverse spin-freezing below  $T_{xy}$ , and hence an asperomagnetic structure with a random anisotropic distribution of moment directions, and in this way a non-zero

magnetization within a domain.

Sputtered samples can be produced by different treatments such as DC and rf sputtering as well as co-sputtering. The magnetic properties of samples produced by each of these sputtering methods should be analysed separately since the configuration of the magnetic or structural inhomogeneities in each type of sample could produce different results and add further controversy to this difficult research field. Mössbauer measurements [25, 26] on sputtered amorphous  $Fe_xZr_{100-x}$  within the Fe-rich region and the intermediate-concentration range also show an increase in the linewidth at around  $T_{xy}$ , indicating that one of the above two models should be applicable.

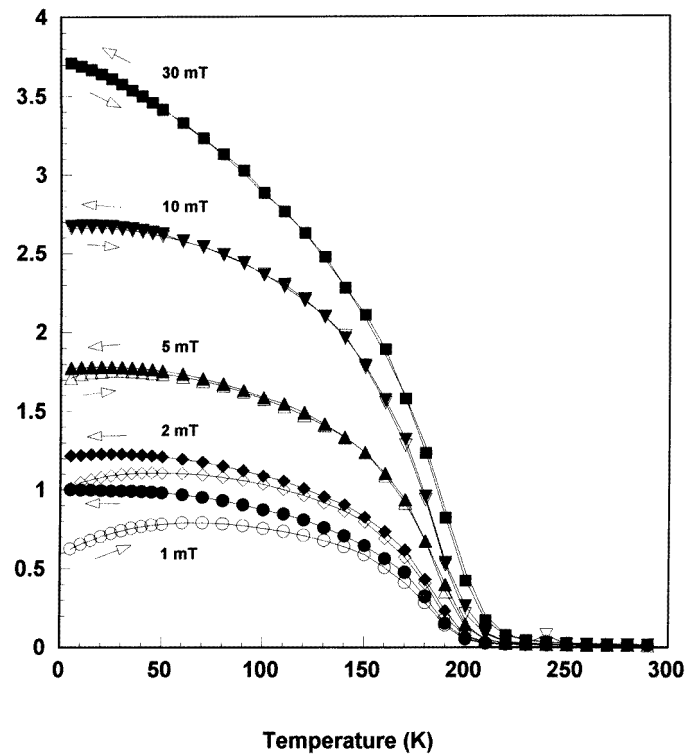
DC-sputtered  $Fe_xZr_{100-x}$  amorphous alloys within the composition region  $55 \leq x \leq 88$  have been considered [4, 5] as behaving as normal ferromagnets even at low temperatures, although samples in this region show a much larger high-field susceptibility as compared with a normal ferromagnet. On the other hand, the decrease of the AC susceptibility [4] and magnetization [5] at low temperatures for the samples within the range  $50 \leq x \leq 55$  have been interpreted as indicating a re-entrant behaviour (paramagnetic–ferromagnetic–spin-glass transition) in a dilute-cluster spin-glass region,  $50 \leq x \leq 55$ . A percolation limit is suggested for  $x = 50$ , and the magnetic properties for samples within the composition range  $35 \leq x \leq 50$  have only been reported for melt-spun samples. The behaviour in this region is that of a superparamagnet, since the magnetization curves for different temperatures appear to approach very closely to the Langevin function, and the coercivity disappears above  $T_{xy}$ .

This communication is the latest in a series of reports on the same  $Fe_xZr_{100-x}$  rf-sputtered amorphous samples involving magnetic properties [17], anomalous Hall effect measurements [27], electrical resistivity [28] and Mössbauer measurements [26]. Our aim is to explore the variation of the magnetic structure with composition in a way which can help to distinguish between the two proposed models, and allow a magnetic phase diagram to be proposed.

## 2. Experimental details

Amorphous  $Fe_xZr_{100-x}$  thin films ( $86 \leq x \leq 40$ ) were grown in Cracow. The samples were deposited by rf sputtering onto water-cooled quartz and glass substrates. The experimental details have been described elsewhere [17]. Films were produced from Fe–Zr composite targets; the targets consisted of square Zr pieces, of approximate area  $5 \text{ mm}^2$ , symmetrically placed on an 80 mm diameter Fe disc. The thicknesses of the deposited films were typically between 850 nm and 1100 nm as determined from step profiling. The composition of the samples was measured by energy-dispersive x-ray fluorescence to an accuracy of about 1%. The compositional homogeneity was checked by Auger electron spectroscopy depth profiling. The homogeneity of the amorphous state was checked by conversion-electron Mössbauer spectroscopy [21] and x-ray diffraction.

Magnetic measurements were made in fields up to 5 T and at temperatures from 5 to 300 K using a Quantum Design MPMS SQUID magnetometer on samples with Fe concentrations given by  $x = 40, 44, 52, 60, 64$ . Magnetic fields could be set to an accuracy of  $\pm 10^{-6}$  T and temperatures to within  $\pm 10^{-2}$  K. Two types of magnetic measurement were made: (a) measurements of partial hysteresis loops in fields covering the range  $-100 \text{ mT} \leq \mu_0 H \leq 5 \text{ T}$  and over a wide range of temperatures, (b) zero-field-cooled/field-cooled (ZFC/FC) measurements in applied fields within the range  $1 \text{ mT} \leq \mu_0 H \leq 30 \text{ mT}$ . The temperature was stepped in 2 K or 5 K increments over the range where the magnetization was rapidly varying. From the hysteresis loop measurements, we were

$$M(T)/M(5\text{ K}, 1\text{ mT})$$


**Figure 1.** Temperature dependences of the normalized magnetization of an amorphous  $\text{Fe}_{64}\text{Zr}_{36}$  rf-sputtered thin film for applied fields of 1 mT, 2 mT, 5 mT, 10 mT and 30 mT. ZFC measurements are represented by open symbols and FC ones by solid symbols.

able to determine coercivities and saturation moments. The Curie temperatures of the samples investigated were estimated from the magnetization plots. In order to correct for the diamagnetic contribution of the substrate, a sample was first measured as described above and then the film was removed from the substrate by dissolving it in acid. The remaining substrate was then re-measured using the same programme as previously used for the whole sample.

### 3. Results

Figure 1 shows the ZFC/FC measurements of the magnetization of the sample  $\text{Fe}_{64}\text{Zr}_{36}$  for different constant applied fields. When the applied field is small ( $\mu_0 H \leq 5$  mT), the heating curves (ZFC) and the cooling curves (FC) bifurcate at a value determined by the field strength. For applied fields larger than 10 mT there is a considerable magnetization induced and the splitting between the ZFC and the FC curves disappears. ZFC curves obtained for low applied fields in this sample show a maximum at a temperature which we describe as  $T_{xy}$  in line with other workers. Below this maximum we choose to interpret the magnetization decreases as being due to non-collinear spin arrangements. The irreversibility in the low-field measurements, between the ZFC and the FC curves, appears for temperatures

close to the Curie temperature.

The units of the magnetization have been chosen to be dimensionless to avoid error associated with the determination of a precise value of the mass or the volume of the samples. In any case, the point to be made is that experimental results show that the ZFC curves of these amorphous alloys show a maximum, and in this way the scale of the magnetization axis is irrelevant.

Figure 2 shows the magnetization behaviour for rf-sputtered  $Fe_xZr_{100-x}$  amorphous alloys as a function of composition within the range  $64 \leq x \leq 40$  for a small constant applied field of 1 mT. Within the range  $64 \leq x \leq 44$ , all ZFC curves show a maximum.

It is not clear from the present experimental results whether or not the sample with composition  $x = 40$  will show a maximum for temperatures below 5 K, although the values of the spin-freezing temperature seem to decrease monotonically, suggesting that  $T_{xy}$  could be about 5 K for this sample.

The Curie temperatures were estimated from the minima of the plots of  $dM/dT$  versus  $T$  using the low-field ZFC data. Figure 3 gives a typical example for an alloy of the composition with  $x = 52$ .

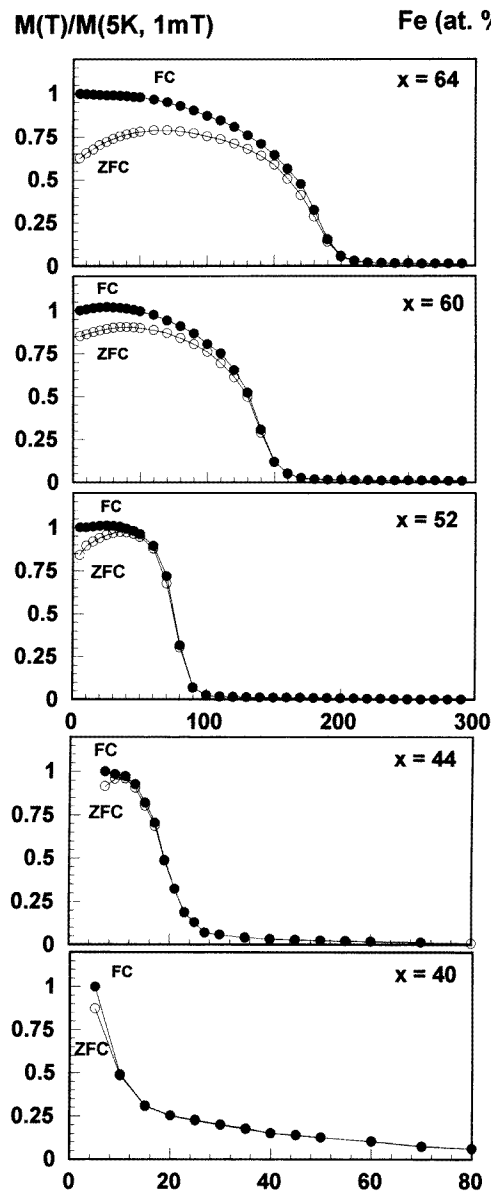
Table 1 shows the values of the Curie temperature extracted from the present data, the spin-freezing temperatures ( $T_{xy}$ ), the magnetic moment at 5 K and the coercivity as measured at 5 K. The exact determination of the spin-freezing temperature is still not clear because of its field dependence, although the values in table 1 can be considered as reasonable data due to the small variation of  $T_{xy}$  for low applied fields.

**Table 1.** A summary of the data determined.

	$Fe_{64}Zr_{36}$	$Fe_{60}Zr_{40}$	$Fe_{52}Zr_{48}$	$Fe_{44}Zr_{56}$	$Fe_{40}Zr_{60}$
$T_C$ (K)	$180 \pm 2.5$	$140 \pm 2.5$	$80 \pm 2.5$	$25 \pm 1.5$	$10 \pm 2.5$
$T_{xy}$ (K) ( $\mu_0 H = 1$ mT)	$60 \pm 2.5$	$40 \pm 2.5$	$25 \pm 2.5$	$10 \pm 2.5$	
Magnetic moment ( $\mu_B$ ) ( $T = 5$ K)	0.97	0.82	0.63	0.28	0.14
$\mu_0 H_C$ (mT) ( $T = 5$ K)	0	0	3.5	14.2	3.6

#### 4. Discussion

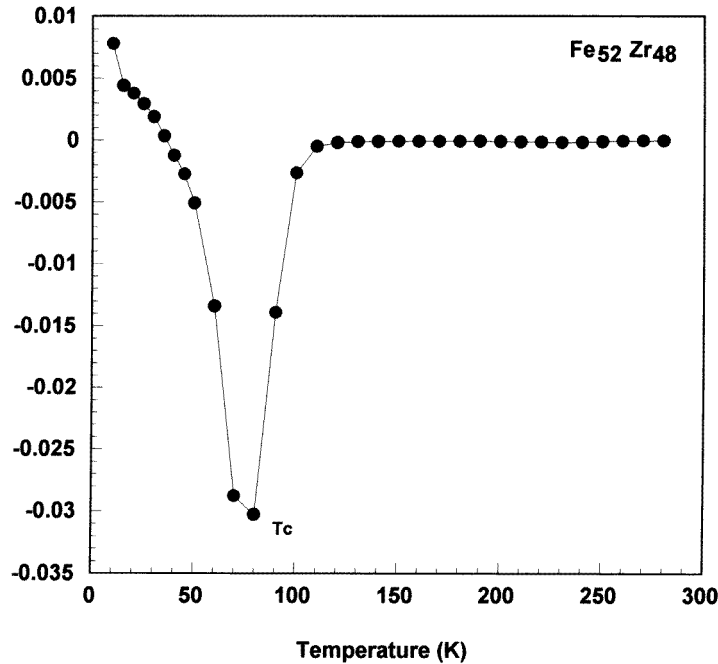
The experimental results in figure 1 and the high-field susceptibility at low temperatures reported previously [17] for the same sample indicate that the alloy  $Fe_{64}Zr_{36}$  does not exhibit ideal ferromagnetic behaviour at low temperatures. This thermo-magnetic history could be caused by intrinsic coercive-field-type effects assuming a random-directional local anisotropy field model [29], but Fe–Zr amorphous alloys do not have such a large anisotropy field and  $T_{xy}$  can be regarded as a spin-freezing temperature. Similar behaviour is observed for samples with higher Zr concentrations, and the decrease in the magnetization for all these samples below a certain temperature  $T_{xy}$  is clear, in figure 2, for a low applied field ( $\mu_0 H = 1$  mT).



**Figure 2.** ZFC (open circles)/FC (solid circles) behaviour, with a steady applied field of 1 mT, of rf-sputtered  $Fe_xZr_{100-x}$  amorphous thin films with Fe concentrations given by  $x = 64, 60, 52, 44, 40$ . Solid lines are shown as a guide to the eye.

The values obtained for the Curie temperatures,  $T_C$ , by the method employed in this paper differ slightly from those determined earlier by anomalous Hall effect measurements on the same samples [27], but agree with those obtained by Mössbauer measurements by other workers [3]. This is entirely attributable to the different extrapolation methods used in the determination of this critical temperature.

On the basis of the present results, we are able to propose a tentative magnetic phase

$$d(M(T) / M(5K, 1mT)) / dT$$


**Figure 3.** The derivative of the normalized magnetization as a function of the temperature for amorphous  $Fe_{52}Zr_{48}$  rf-sputtered thin film.

diagram for rf-sputtered  $Fe_xZr_{100-x}$  amorphous alloys within the intermediate range. In this diagram the temperatures of the spin-freezing transition,  $T_{xy}$ , have been included. A similar type of magnetic phase diagram has been reported for several other Fe-based amorphous alloys such as Fe–Lu, Fe–Ce and Fe–Y [13]. The present diagram seems to be consistent with that corresponding with the Fe-rich region of rf-sputtered  $Fe_xZr_{100-x}$  amorphous alloys [3].

From the discussion in the introduction, the reduction in the magnetization below  $T_{xy}$  can be considered as being due to either the appearance of an asperomagnetic behaviour or to a cluster behaviour. The samples  $Fe_{64}Zr_{36}$  and  $Fe_{60}Zr_{40}$  show no coercivity over the entire range of measurement temperatures, within the field resolution of the SQUID. Other workers [4, 5] have found the same result on melt-spun and DC-sputtered samples, and have interpreted this behaviour as ruling out the presence of clusters. If we accept this interpretation, in these two samples the magnetic state below  $T_{xy}$  can best be described as an asperomagnetic one. The coercivity disappears in the range  $10 < T < 15$  K for the samples  $Fe_{52}Zr_{48}$  and  $Fe_{44}Zr_{56}$ . The temperatures at which the coercivity disappears are below  $T_{xy}$  for these compositions. The coercivity of the sample  $Fe_{40}Zr_{60}$  disappears for  $5 < T < 10$  K, and this temperature is above  $T_{xy}$ .

The disappearance of coercivity could be interpreted as the appearance of a percolation limit at  $x = 50$  (as previously reported [5] for amorphous  $Fe_xZr_{100-x}$  DC-sputtered samples), above which the behaviour would be that of a superparamagnet. However, the disappearance of coercivity cannot be associated with  $T_{xy}$  as these are different for all alloys studied.



## Temperature (K)

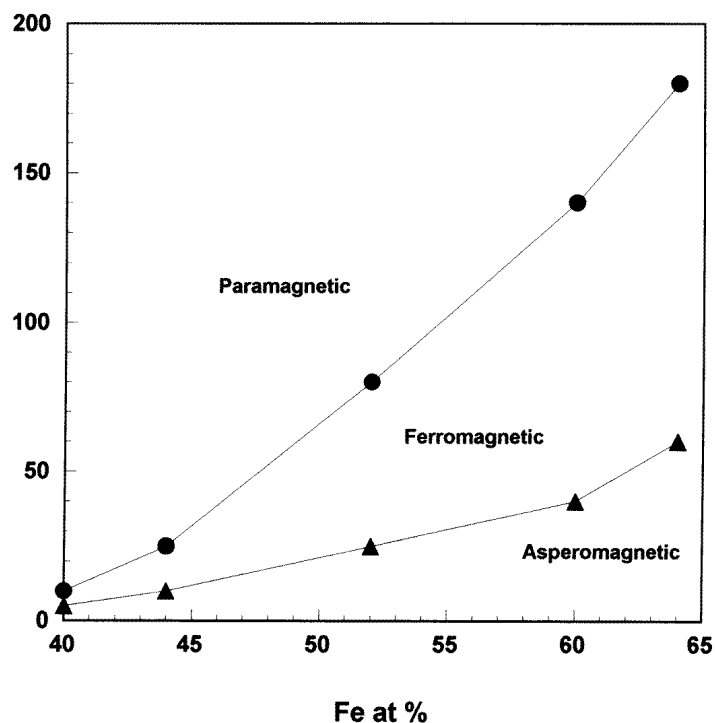


**Figure 4.** A tentative magnetic phase diagram for rf-sputtered  $\text{Fe}_x\text{Zr}_{100-x}$  amorphous thin films within the range  $64 \leq x \leq 40$ . Solid circles represent the values of  $T_C$  and solid triangles the values of the transverse spin-freezing transition  $T_{xy}$ .

The monotonic decrease of  $\mu$ ,  $T_C$  and  $T_{xy}$  with decreasing Fe concentration across the whole composition range ( $64 \leq x \leq 40$ ), for the results reported here, strongly implies that structural changes do not occur throughout the whole temperature range below  $T_C$ . That is, we do not see any evidence of cluster formation, or significant changes in short-range order. Durand [30] has reviewed compositional data for a wide range of amorphous alloys, and sees no discontinuities.

With all the above, we conclude that a transition to an asperomagnetic state is detected below  $T_{xy}$  for all of the samples investigated, and that the onset of coercivity comes from another mechanism. The appearance of coercivity at lower Fe concentrations requires an alternative explanation to that of clustering or superparamagnetism.

The decrease in Curie temperature may reflect a decrease in the exchange coupling; the Fe-Fe distance is known to be distributed in amorphous alloys [30]. As exchange weakens, the random local anisotropy may dominate more, and spins freeze out at higher temperatures. Thus for the Fe-rich samples, exchange dominates the anisotropy over the entire temperature range, whereas at lower Fe concentrations, significant spatial fluctuations of the magnetization vector may appear at low temperatures. This can give rise to intrinsic coercivity [31].

Non-collinear magnetic structures such as asperomagnetism, speromagnetism and

sperimagnetism occur in amorphous alloys [32], but Fe–Zr amorphous alloys have been regarded by some workers [6, 8, 19, 20] as possessing a spin structure that is unique to these amorphous alloys. In this spin structure the ferromagnetic alignment is limited to clusters of some nanometres in extent, although the experimental proof of a true phase separation between these clusters is still lacking. Conversion-electron Mössbauer spectroscopy measurements of amorphous  $Fe_xZr_{100-x}$  sputtered samples, showing changes in the linear temperature dependence of the hyperfine field with and without applied field, would be most informative. We have found no evidence for cluster formation in our compositional dependence of the Curie temperature or moment, and a critical temperature below which the thermo-magnetization behaviour implies an asperomagnetic spin structure.

## 5. Conclusions

Magnetic measurements have been performed on a series of rf-sputtered amorphous  $Fe_xZr_{100-x}$  samples with  $x$  in the range  $64 \leq x \leq 40$ . The appearance of an asperomagnetic state is proposed for all of the samples investigated. This conclusion is supported on the basis that there is no evidence of structural inhomogeneity in these alloys. The appearance of coercivity in low-Fe-concentration alloys may be tentatively ascribed to a competition between exchange and anisotropy on the local scale.

## Acknowledgment

One of us (FJC) would like to thank Dr T Moyo of the University of Natal (South Africa) for helpful discussions.

## References

- [1] Hiroyoshi H and Fukamichi K 1981 *Phys. Lett.* **85A** 242
- [2] Altounian Z and Ström-Olsen J O 1983 *Phys. Rev. B* **27** 4149
- [3] Unruh K M and Chien C L 1984 *Phys. Rev. B* **30** 4968
- [4] Saito N, Fukamichi K and Nakagawa Y 1990 *Sci. Rep. Res. Inst. Tohoku Univ. A* **35** 65
- [5] Hiroyoshi H, Fukamichi K and Nakagawa Y 1986 *Sci. Rep. Res. Inst. Tohoku Univ. A* **33** 68
- [6] Vincze I, Kaptas D, Kémény T, Kiss L F and Balogh J 1994 *Phys. Rev. Lett.* **73** 496
- [7] Fukamichi K, Goto T, Komatsu H and Wakabayashi H 1989 Spin glass and Invar properties of iron-rich amorphous alloys *Physics of Magnetic Materials* ed W Gorzkowski, H K Lachowicz and H Szymczak (Singapore: World Scientific) p 354
- [8] Read D A, Moyo T, Jassim S, Dunlap R A and Hallam G C 1989 *J. Magn. Magn. Mater.* **82** 87
- [9] Ryan D H, Coey J M D, Batalla E, Altounian Z and Ström-Olsen J O 1987 *Phys. Rev. B* **35** 8630
- [10] Nicolaides G K and Rao K V 1993 *J. Magn. Magn. Mater.* **125** 195
- [11] Krompiewski S, Krey U and Krauss U 1989 *Phys. Rev. B* **39** 2819
- [12] Wohlfarth E P 1983 Itinerant electron model of magnetic properties *Amorphous Metallic Alloys (Butterworths Monographs in Materials)* ed F E Luborsky (London: Butterworths) pp 289–99
- [13] Yu M, Kakehashi Y and Tanaka H 1994 *Phys. Rev. B* **49** 352
- [14] Ma H, Kundel H P and Williams G 1991 *J. Phys.: Condens. Matter* **3** 5563
- [15] Kiss L F, Kémény T, Vincze I and Gránásy L 1994 *J. Magn. Magn. Mater.* **135** 161
- [16] Gabay M and Toulouse G 1981 *Phys. Rev. Lett.* **47** 201
- [17] Kossacki P, Stobiecki T and Szymczak H 1993 *Acta Phys. Pol. A* **83** 785
- [18] Lorenz R and Hafner J 1995 *J. Magn. Magn. Mater.* **139** 209
- [19] Moyo T 1996 *J. Magn. Magn. Mater.* **154** 201
- [20] Kaptas D, Kémény T, Kiss L F, Balogh J, Gránásy L and Vincze I 1992 *Phys. Rev. B* **46** 6600
- [21] Jacobs I S and Bean C P *Fine particles, Thin Films and Exchange Anisotropy (Effects of Finite Dimensions and Interfaces on Basic properties of Ferromagnets)* (New York: General Electric Research Laboratory)

- [22] Hiroyoshi H and Fukamichi K 1982 *J. Appl. Phys.* **53** 2226
- [23] Ryan D H, Ström-Olsen J O, Provencher R and Townsend M 1988 *J. Appl. Phys.* **64** 5787
- [24] Ryan D H and Hong Ren 1991 *J. Appl. Phys.* **69** 5057
- [25] Fries S, Crummenauer J, Wagner H G and Gonser U 1988 *Z. Phys. Chem., NF* **157** S127
- [26] Przybylski M, Krop K, Stobiecki T and Dargel-Sulir L 1986 *Hyperfine Interact.* **27** 425
- [27] Karas W and Stobiecki T 1987 *J. Magn. Magn. Mater.* **69** 253
- [28] Paja A and Stobiecki T 1986 *Phys. Status Solidi b* **134** 331
- [29] Rhyne J J, Schelleng J H and Koon N C 1974 *Phys. Rev. B* **10** 4672
- [30] Durand J 1983 *Glassy Metals II* ed H Beck and H-J Guntherodt (Berlin: Springer) p 343
- [31] Evetts J E, Howarth W and Gibbs M R J 1979 *Proc 3rd Int. Conf. on Rapidly Quenched Metals (Brighton, 1978)* vol 2 (London: The Metals Society) p 127
- [32] Hansen P 1991 Magnetic amorphous alloys *Handbook of Magnetic Materials* vol 6, ed K H J Buschow (Amsterdam: Elsevier) p 320